WILEY-VCH

# Bio-based wrinkled surfaces harnessed from biological design principles of wood and peroxidase activity

Hironori Izawa,*[a] Noriko Okuda,[a] Shinsuke Ifuku,[a] Minoru Morimoto,[a] Hiroyuki Saimoto,*[a] and Orlando J. Rojas[b], [c]

**Abstract:** A new and simple approach for surface wrinkling inspired by polymer assemblies in wood fibers is introduced. A hard skin is synthesized on a linear polysaccharide support that resembles the structural units of the cell wall. This skin, a wood mimetic layer, is produced via immersion in a solution containing phenolic precursor and subsequent surface reaction by horseradish peroxidase. A patterned surface with micron-scale wrinkles is formed upon drying and as a result of inhomogeneous shrinkage. We demonstrate that the design of the micro-structured surface can be controlled by the molecular structure of the phenolic precursor, temperature and drying stress. It is noteworthy that this is a totally bio-based system involving green materials and processes.

Nature has evolved excellent functional surfaces that take advantage of hierarchical structures based on commonly found materials.[1] Biological surface can thus be imitated via self-assembly to provide desirable properties and to develop innovative materials and devices.[2]

Surface wrinkling is a physical process that is responsible for the formation of many intriguing surface architectures displayed by plants and animals.[3] This spontaneous process is the result of inhomogeneous changes triggered by internal stresses and swelling/shrinking of tissue layers possessing different elastic moduli and reacting to gradients in temperature, humidity, etc.[3b] The critical process in surface wrinkling, to enable given functions in nature, can be conducted artificially in order to design microscopic surface features for optical[4] and electronic devices[5], to attain tunable wettability[6] and adhesion[7] and to synthesize cell culture scaffolds.[8] For example, UV/O$_3$ treatment is typically used to form a hard layer on a film of strained poly(dimethylsiloxane), which is subsequently released to produce surface wrinkling via inhomogeneous shrinking.[3a, 9] Although many sophisticated systems have been introduced in

the development of surface wrinkling, the basic approach remains the same: fabrication of a hard thin (skin) layer on a soft support via dry processing, including chemical vapor deposition[10], photo-crosslinking[11], and UV/O$_3$ oxidation[9]. The available materials for surface wrinkling are thereby limited and they often demand specialized, electrically-powered devices to fabricate the skin layer or to control material stress. Therefore, a current, pressing need in this field is to develop new approaches for the synthesis of hard thin layers that enable flexible material design and versatility. An environmentally benign approach is naturally preferable.

Higher plants in the biosphere have evolved into robust and complex organizations that carry multiple functions. Lignin, a key component generating in woods, forms a crosslinked macromolecular structure based on phenylpropanoid units that adds strength and rigidity to the fiber's cell walls.[12] Lignin is produced by a natural process, lignification, in which precursor molecules are polymerized and immobilized biocatalytically on heteropolysaccharides via peroxidase and laccase enzymes.[13] This process inspired this contribution aimed to develop a novel surface wrinkling system by means of wet processing and using horseradish peroxidase (HRP)[14] (Figure 1). The biomimetic approach stands on the basis of the formation of a hard skin layer via crosslinking on a polysaccharide support, similar to lignification in wood. The HRP-catalyzed crosslinking of a tyrosine containing peptide with ferulic acid has been reported.[15] In addition, surface wrinkling by means of a surface reaction in wet conditions has been attempted.[16] However, the utilization of wood-like components, as a biomimetic multilayer deposition in the cell wall has not been considered. Likewise, water evaporation during film consolidation to trigger surface wrinkling has hardly been considered.[16c, 17] Therefore, despite the fact that related processes are ubiquitous in nature[3b], it is surprising that they have not been exploited. Herein, we introduce a new approach for surface wrinkling, inspired by wood.

[a] Dr. H. Izawa, N. Okuda, Dr. S. Ifuku, Dr. M. Morimoto, Dr. H. Saimoto
Graduate School of Engineering
Tottori University
4-101 Koyama-Minami, Tottori 680-8550 (Japan)
E-mail: h-izawa@chem.tottori-u.ac.jp
saimoto@chem.tottori-u.ac.jp
[b] Dr. O. J. Rojas
Biobased Colloids and Materials (BiCMat), School of Chemical Technology
Aalto University
P. O. Box 16300, FIN-00076 Aalto (Finland)
[c] Dr. O. J. Rojas
Departments of Forest Biomaterials and Chemical and Biomolecular Engineering
North Carolina State University
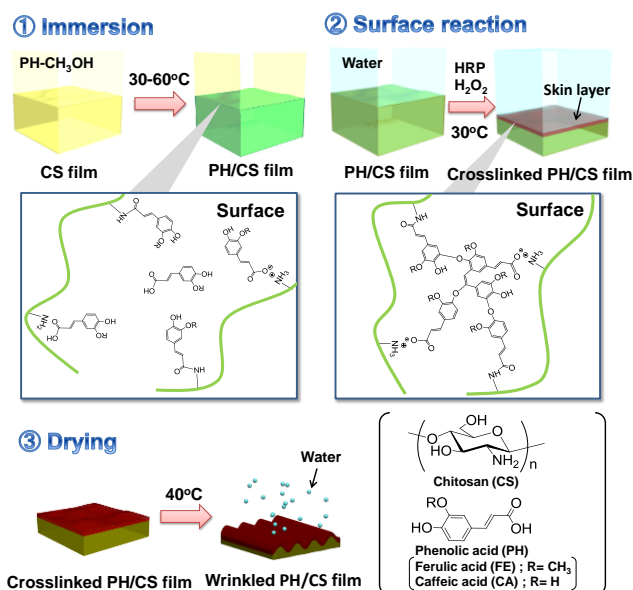Raleigh, North Carolina 27695-8005 (United States)

Supporting information for this article is given via a link at the end of

**Figure 1.** Schematics illustrating the wood-inspired surface wrinkling systems used in this study.

The wood-inspired wrinkling system presented here uses chitosan (CS) and a phenolic acid (PH) as precursors for polysaccharide and lignin, respectively. This is to take advantage of electrostatic complexation between CS and PH, which enhances adsorption and binding. We take advantage of known HRP-catalyzed reactions of PHs such as ferulic acid (FE)[15] and caffeic acid (CA)[18] that are carried out in aqueous media. Besides, these materials are obtained from natural resources. Remarkably, preliminary experiments revealed the formation of covalently bound FE on the CS film via amide bond, which was facilitated by simple immersion of the CS film into FE methanolic solution. Figure 2C shows $^1$H NMR spectra of the aromatic region of a FE/CS film prepared though immersion in FE methanolic solutions at 50 °C for 24 h. The spectra show the signals attributed to the adsorbed FE, including a signal **a** slightly shifted to lower magnetic field, suggesting ionic bonding between CS and FE. Moreover, some signals, not shown in the FE spectrum, developed in FE/CS suggested the occurrence of chemical coupling (covalent bonding). For confirmation, the FE/CS film was Soxhlet-extracted with methanol for 1 week in order to remove any unreacted FE. Figure 2B shows the $^1$H NMR spectrum of the extracted FE/CS film. In the spectrum, the contribution of FE is mostly absent but new signals, not observed in the FE sample, developed at 6.0, 6.5, and 7.0 ppm. They suggest covalently-bound FE. A dehydration condensation between CS and FE is possible given that the 6.0 and 6.5 ppm peaks shown in the extracted FE/CS film correspond to shifted contribution of protons **a** and **e** via amide formation. In order to confirm this hypothesis, we prepared a reference sample consisting of FE-grafted to CS (Scheme S1), which carry covalently-bound (amide bond) FE. Figure 2A shows the $^1$H NMR spectrum of the aromatic region of FE-grafted CS. In the spectrum, signals at 6.0 (f) and 6.5 (g) ppm are shown as well as that in the extracted FE/CS film, which indicate the presence of covalently-bound FE in the FE/CS film. The dehydration condensation reaction under mild condition is unexpected. However, it is possible that amides are formed at the CS interface through ester exchange since a small amount of methyl ester of FE or CA is generated, owing to the presence of large amounts of methanol (Scheme S2). Thus, the occurrence of dehydration condensation reaction between CS and FE is proposed to occur during the immersion process. Following, we hypothesized the other covalently bound PHs are generated by a Michael-type addition[19] of a primary amine to a α,β-unsaturated carboxylic acid moiety. Note that $^1$H NMR analysis of the CA/CS film was difficult due to the reactions involving catechol moieties. The reactions involved with catechol moieties in CA/CS film include Schiff-base products and/or Michael-type additions (Scheme S3).[20]

These covalently bound PH can work as reaction sites on the CS film for the HRP-catalyzed crosslinking and to form a skin layer, as shown in Figure 1. C/N ratios measured for the CS films after immersion into FE or CA methanolic solutions at 30-60 °C for 24 h (FE/CS or CA/CS films) as well as soxhlet-extracted (methanol, 1 week) films (Extracted FE/CS or Extracted CA/CS films) are shown in Figure 3. In the case of Extracted FE/CS films, the C/N ratios are shown to gradually increase with the immersion temperature, indicating that covalent binding of FE increases with temperature during the immersion process. The C/N ratios are higher for the Extracted CA/CS films compared to those for FE/CS. This is probably due to reactions involving catechol moieties. The adducts cannot work as reaction sites for the HRP-catalyzed crosslinking because of the substrate specificity of the HRP. Therefore, in the case of CA, the C/N ratios of the Extracted CA/CS films do not directly reflect the amount of the reaction sites on the CS film.
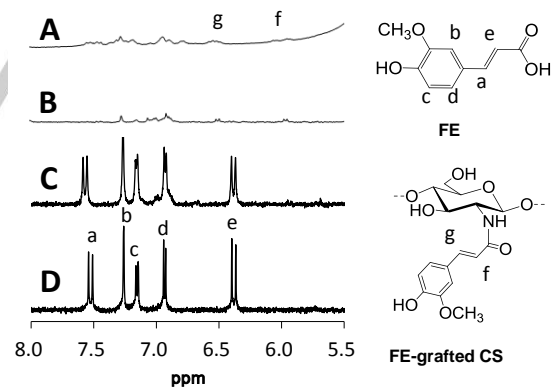


**Figure 2.** $^1$H NMR spectra of aromatic region of the synthesized FE-grafted CS (A), the extracted FE/CS film (B), FE/CS film (C), and FE (D) in 1% $CD_3COOD$-$D_2O$.
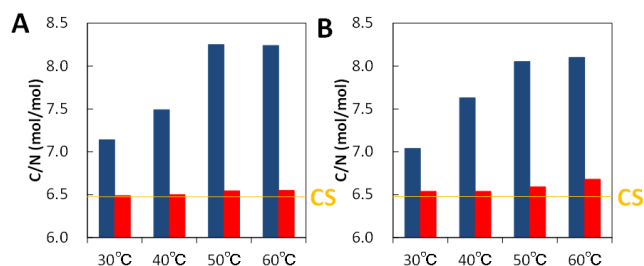
**Figure 3.** C/N ratios (CHN elemental analysis) of films obtained by binding two phenolic acids (PH) on CS: FE (A) and CA (B). Included are PH/CS films (blue bars) and Extracted PH/CS films (red bars). The horizontal reference line indicates the C/N ratio for the bare CS support.
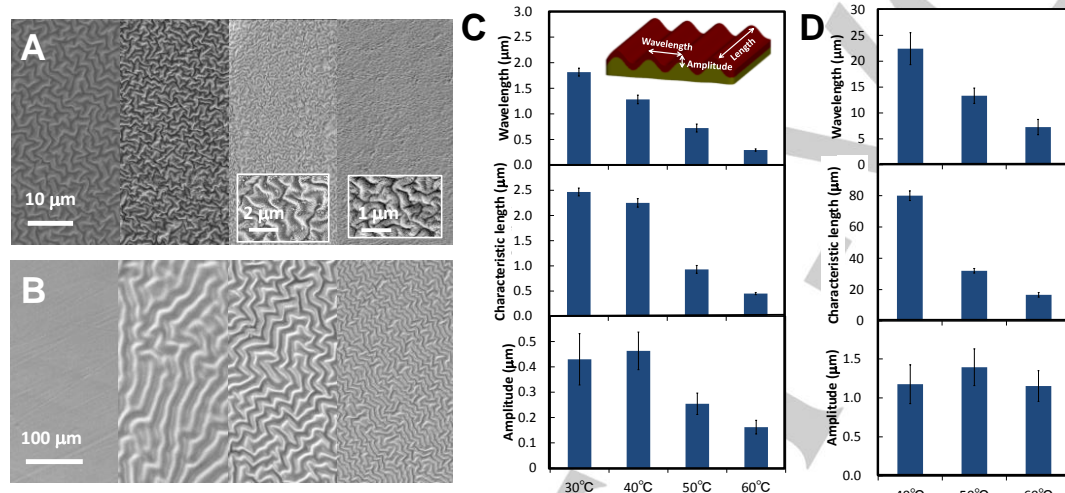


**Figure 4.** Plane view SEM images of films obtained with FE (A) and CA (B) (FE/CS and CA/CS) by using different immersion temperatures (30, 40, 50, 60 °C from left). The mean wavelength, characteristic length, and amplitude of wrinkles formed in FE/CS (C) and CA/CS (D) films upon immersion at given temperatures are indicated. The characteristic length is defined as a length between distinct folding points. The amplitudes were measured by SPM analysis.

The FE/CS and CA/CS films prepared through immersion at 30-60 °C were subjected to HRP-catalyzed crosslinking just after the immersion, thereby forming a wood mimetic skin layer. Subsequently, the composite films were dried at 40 °C (50% relative humidity). Figure 4A and B show SEM plane view images of the surface of the composite films. Detailed characterization of the wrinkles formed is available in Figure 4C and D. By using FE, unordered wrinkles were formed in all cases. At an immersion temperature of 30 °C, the mean wrinkle wavelength, characteristic length, and amplitude were 1.8, 2.5, and 0.4 μm, respectively. These gradually decreased with treatment at increased temperatures. When CA was used, wrinkling was observed on CA/CS film for immersion temperatures above 40 °C. No wrinkling occurred at 30 °C. This is probably due to the lack of crosslinking reaction sites on the CA/CS film. It is likely that the reactions to generate the reaction sites in the CA/CS system are slower than that of the FE/CS system. With respect to the morphology, the mean wrinkling wavelength, characteristic length, and amplitude at 40 °C immersion are much larger (22.4, 80.0, and 1.2 μm,

respectively) than those measured for FE/CS film. The mean wrinkling wavelength and characteristic length decreased gradually as the temperature increased, as was the case in FE/CS systems. These results clearly indicate that the immersion process plays a crucial role in wrinkling development. A possible reason for the characteristic scaling of wrinkles size with immersion temperature is the difference in the amount of the reaction sites for the HRP-catalyzed crosslinking as described above; the larger quantity of the reaction sites generated at higher immersion temperature leads to the production of a harder skin layer, which leads to a smaller wrinkling wavelength because of stronger shrinking. The morphological differences observed for FE/CS and CA/CS systems are most likely due to the differences in the moduli of FE and CA skin layers compared to that of the supporting CS.[3, 21] Indeed, the modulus of the CA/CS or the Wrinkled CA/CS film is much higher than that of the respective FE/CS films, as determined by the reactions involving the catechol moieties (see the supporting information). The comparable amplitudes shown in the CA/CS system is also probably associated with the higher moduli. A detailed study on the relationship between wrinkle structure and layer moduli is in progress. In passing, it is worth mentioning that wrinkles were not formed in systems that included a catechol which did not carry the α,β-unsaturated carboxylic acid. This highlights the important role of the α,β-unsaturated carboxylic acid to induce surface wrinkling.

SEM observations of the cross sections of the films were not suitable to discern the skin layer from the CS support (Figure S4). Therefore, in order to confirm the formation of such layer, *in situ* quartz crystal microgravimetry with dissipation monitoring (QCM-D) was applied to investigate the formation of the skin layer in real time (Figure 5 for CA/CS systems). Here, the shift in the resonance frequency ($\Delta f$) is directly related to the change in interfacial mass while the shift in energy dissipation ($\Delta D$) indicates changes in layer viscoelasticity. First, QCM sensors with pre-adsorbed CS thin films were immersed in CA-methanol solution for 24 h either at 30 or 50 °C. Subsequently, they were rinsed in methanol background solvent to remove weakly adsorbed CA and dried in air. After placing the sensors in the QCM module, the difference in the frequency of vibration ($\Delta f$) was measured in air. The $\Delta f$ measured for samples prepared at 50 °C (-20.3 Hz) and 30 °C (-5.5 Hz) indicated a larger amount of CA bound to the CS support when the higher immersion temperature was used. Water was injected in the QCM module on the sensor coated with the CA/CS film and until reaching a steady frequency signal, at which point the $f$ value was set to zero. This, as well as the following experiments were conducted

at constant temperature of 30 $^{\circ}$C. Experiments with HRP addition were carried out, as explained next. After ~10 min equilibrium QCM data acquisition in water, either an "active solution" (containing CA, HRP and $H_2O_2$) or a CA-free solution (containing HRP and $H_2O_2$ only) was injected into the system. Successful skin layer formation was observed for the sensors that were prepared at 50 $^{\circ}$C and upon introduction of the active solution (blue profile, Figure 5): $\Delta f$ sharply decreased after 11 min, indicating adsorption of CA, HRP, and $H_2O_2$. Then, $\Delta f$ temporarily increased (at times from 11.5 to 12.5 min), suggesting removal of coupled water from the CA/CS film, as a consequence of HRP-catalyzed crosslinking. The $\Delta D$ signal distinctly decreased after injection of the active solution, indicating hardening and/or thinning of the layer. Similar changes in QCM sensograms have been reported during crosslinking of a protein film.[22] The distinctive changes in $\Delta f$ and $\Delta D$ noted upon injection of the active solution were not observed in experiments using a sensing element that was prepared at 50 $^{\circ}$C but with CA-free solution (yellow profile, Figure 5). No skin layer formation was registered when active solution was injected in the QCM module containing the sensor prepared at 30 $^{\circ}$C (red profile, Figure 5). Despite the transient change in $\Delta f$ (time from 13.5 to 22.0 min), which suggests removal of coupled water, a positive $\Delta D$ shift was observed. Thus, a soft layer was formed, which proved not to be suitable to induce surface wrinkling, as demonstrated by the unsuccessful wrinkling at 30 $^{\circ}$C (Figure 4B). Taken all together, there is evidence of the formation of a skin layer catalyzed by HRP when CA is present in the system and provided a high enough temperature is used in the preparation of the CA/CS substrate carrying the reaction sites.

In order to analyze the outer layers, ATR-IR spectra of the film surfaces were acquired (Figure S5) and indicated the presence of ionic bonding between polyPHs produced by the surface reaction and CS; also, it confirmed composites composed of the polyPHs and CS, as shown in Figure 1. Moreover, it is concluded that polyPHs involved in the outer layers are oligomeric as can be confirmed by MALDI-TOF MS analysis of products prepared by the HRP-catalyzed reaction of FE and CA under the same condition (Figure S6).
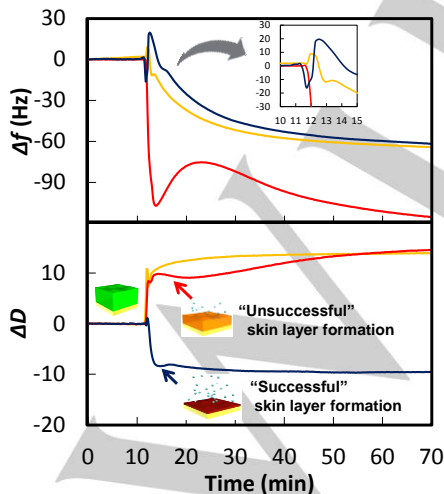


**Figure 5.** QCM-D sensograms registered at 30 $^{\circ}$C to monitor skin layer formation. An experiment simulating a successful skin layer formation with the sensor prepared at 50 $^{\circ}$C was conducted by introducing the active solution, soon after 10 min (blue profile). No skin layer was formed in experiments with the sensor prepared at 30 $^{\circ}$C after introduction of the active solution (red profile). A control experiment with the sensor prepared at 50 $^{\circ}$C and the CA-free solution is included as a reference (yellow profile).

In order to confirm the occurrence of wrinkling during film drying, we directly observed the Crosslinked FE/CS and CA/CS films by using an optical microscope. This was carried out by placing the system in the stage and recording a video to illustrate the morphological changes occurring upon drying under ambient conditions. Figure 6 shows some few captured images (videos are available as supporting video 1 and 2). In both cases, the wrinkles formed gradually with time, upon water evaporation. Based on this observation, it can be predicted that the morphology of the wrinkles can be controlled by drying stress. Thus, we investigated the effect of external stresses. The Crosslinked FE/CS or CA/CS films were clamped and a weight was added to one end and hung for 12 h in air at 40 $^{\circ}$C. Anisotropic wrinkles were observed on the films depending on the direction of application of the stress (Figure 7). These results indicate that vertical surface wrinkling is prevented under elongational stress.
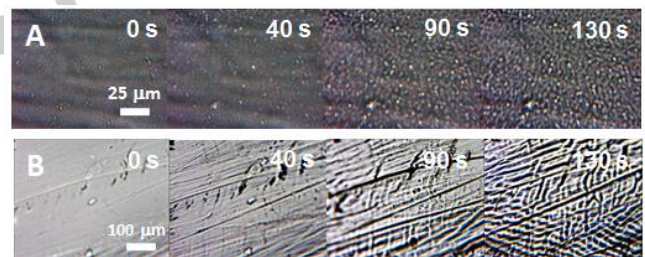


**Figure 6.** Images captured from videos (optical microscopy) during drying of the Crosslinked FE/CS (A) and CA/CS (B).
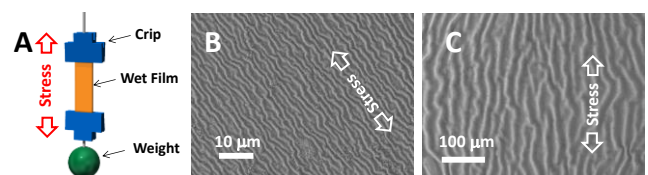


**Figure 7.** Effect of drying under stress (A) on wrinkle formation as assessed by SEM imaging of the surface of FE/CS (B) and CA/CS (C) films. The direction of the stress applied during drying is indicated with the arrows.

Interestingly, we demonstrate that the proposed approaches for wrinkle formation can be produced on the surface of high curvature materials, such as fibers. In fact, surface wrinkling was effective on the surface of CS fibers (Figure S7). Although some reports discuss surface wrinkling on particles[16b, 23] and fibers[24], evidence of surface wrinkling of 3D materials is still quite rare.

In conclusion, we developed a novel surface wrinkling system inspired by wood. Microscopic wrinkles were fabricated on the

surface of CS films and fibers by a facile procedure that involved immersion, surface reaction, and drying. We revealed that the immersion process induce/control surface wrinkling by the formation of covalent bonds between the substrate (CS) and the phenolic acid (PH). PH-bound moieties acted as precursors or reaction sites for crosslinking via HRP-catalyzed polymerization and to yield a skin layer with different elastic modulus compared to the CS support. Further, surface wrinkling was induced by water evaporation during drying. Wrinkling morphology can be controlled by the choice of PH molecular structure, immersion temperature as well as the drying stress applied. The proposed versatile wet processing for wrinkling formation provides the base for designing 3D materials for given functions. It is noteworthy that this is a totally bio-based system involving green materials and processes. Our biomimetic approach has opened the door to wrinkled 3D materials and bio-based wrinkled surfaces.

[1]     B. Bhushan, Y. C. Jung, *Prog Mater Sci* **2011**, *56*, 1-108.

[2]     a) K. Ariga, Y. Yamauchi, G. Rydzek, Q. M. Ji, Y. Yonamine, K. C. W. Wu, J. P. Hill, *Chem Lett* **2014**, *43*, 36-68; b) E. Ruiz-Hitzky, M. Darder, P. Aranda, K. Ariga, *Adv Mater* **2010**, *22*, 323-336.

[3]     a) J. Genzer, J. Groenewold, *Soft Matter* **2006**, *2*, 310-323; b) L. Ionov, *J Mater Chem* **2012**, *22*, 19366-19375.

[4]     T. Ohzono, K. Suzuki, T. Yamaguchi, N. Fukuda, *Adv Opt Mater* **2013**, *1*, 374-380.

[5]     S. G. Lee, H. Kim, H. H. Choi, H. Bong, Y. D. Park, W. H. Lee, K. Cho, *Adv Mater* **2013**, *25*, 2162-2166.

[6]     Y. Y. Li, S. X. Dai, J. John, K. R. Carter, *Acs Appl Mater Inter* **2013**, *5*, 11066-11073.

[7]     C. S. Davis, D. Martina, C. Creton, A. Lindner, A. J. Crosby, *Langmuir* **2012**, *28*, 14899-14908.

[8]     Z. Q. Zhao, J. J. Gu, Y. N. Zhao, Y. Guan, X. X. Zhu, Y. J. Zhang, *Biomacromolecules* **2014**, *15*, 3306-3312.

[9]     K. Efimenko, M. Rackaitis, E. Manias, A. Vaziri, L. Mahadevan, J. Genzer, *Nat Mater* **2005**, *4*, 293-297.

[10]    N. Bowden, S. Brittain, A. G. Evans, J. W. Hutchinson, G. M. Whitesides, *Nature* **1998**, *393*, 146-149.

[11]    C. M. Chen, J. C. Reed, S. Yang, *Soft Matter* **2013**, *9*, 11007-11013.

[12]    W. O. S. Doherty, P. Mousavioun, C. M. Fellows, *Ind Crop Prod* **2011**, *33*, 259-276.

[13]    A. R. Barcelo, *Int Rev Cytol* **1997**, *176*, 87-132.

[14]    N. C. Veitch, *Phytochemistry* **2004**, *65*, 249-259.

[15]    G. Oudgenoeg, R. Hilhorst, S. R. Piersma, C. G. Boeriu, H. Gruppen, M. Hessing, A. G. J. Voragen, C. Laane, *J Agr Food Chem* **2001**, *49*, 2503-2510.

[16]    a) Y. Y. Li, J. J. Peterson, S. B. Jhaveri, K. R. Carter, *Langmuir* **2013**, *29*, 4632-4639; b) J. Yin, X. Han, Y. P. Cao, C. H. Lu, *Sci Rep* **2014**, *4*; c) K. Huraux, T. Narita, B. Bresson, C. Fretigny, F. Lequeux, *Soft Matter* **2012**, *8*, 8075-8081.

[17]    R. Rizzieri, L. Mahadevan, A. Vaziri, A. Donald, *Langmuir* **2006**, *22*, 3622-3626.

[18]    P. Xu, H. Uyama, J. E. Whitten, S. Kobayashi, D. L. Kaplan, *J Am Chem Soc* **2005**, *127*, 11745-11753.

[19]    B. D. Mather, K. Viswanathan, K. M. Miller, T. E. Long, *Prog Polym Sci* **2006**, *31*, 487-531.

[20]    K. M. Gray, E. Kim, L. Q. Wu, Y. Liu, W. E. Bentley, G. F. Payne, *Soft Matter* **2011**, *7*, 9601-9615.

[21]    B. Li, Y. P. Cao, X. Q. Feng, H. J. Gao, *Soft Matter* **2012**, *8*, 5728-5745.

[22]    F. Hook, B. Kasemo, T. Nylander, C. Fant, K. Sott, H. Elwing, *Anal Chem* **2001**, *73*, 5796-5804.

[23]    M. K. Klein, N. R. Saenger, S. Schuetter, P. Pfleiderer, A. Zumbusch, *Langmuir* **2014**, *30*, 12457-12464.

[24]    Y. Zhao, W. M. Huang, Y. Q. Fu, *J Micromech Microeng* **2011**, *21*, 067007.

# COMMUNICATION



**Fully bio-based surface wrinkling systems:** Bio-based wrinkled surfaces were synthesized by using chitosan, ferulic or caffeic acid, and horseradish peroxidase. Wrinkling morphology can be tuned depending on the choice of precursor phenolic compound and coupling conditions.

*Hironori Izawa,\* Noriko Okuda,
Shinsuke Ifuku, Minoru Morimoto,
Hiroyuki Saimoto,\* Orlando J. Rojas*

*Page No. – Page No.*

**Bio-based wrinkled surfaces harnessed from biological design principles of wood and peroxidase activity**